Reduction of Computational Complexity in Simulations of the Flow Process in Transmission Pipelines

Zdzisław Kowalczuk[1], Marek Tatara[1], and Tomasz Stefański[1]

Department of Robotics and Decision Systems,
Faculty of Electronics, Telecommunications and Informatics
Gdańsk University of Technology,
ul. Narutowicza 11/12, 80-233 Gdańsk, Poland,
kova@pg.gda.pl

Abstract. The paper addresses the problem of computational efficiency of the pipe-flow model used in leak detection and identification systems. Analysis of the model brings attention to its specific structure, where all matrices are sparse. With certain rearrangements, the model can be reduced to a set of equations with tridiagonal matrices. Such equations can be solved using the Thomas algorithm. This method provides almost the same values of the state vector and maintains stability for the same discretization grid, while the computational overhead is vastly reduced.

Keywords: flow simulation, numerical analysis, flow process, leak detection and identification

1 Introduction

Simulation of flow processes in transmission pipelines allows one not only to study the behavior of transported fluids but also enables the detection of failures of pipeline installations. Such a simulation can be used to prevent, or quickly react, to leaks in the monitored pipelines. This methodology is widely used in model-based leak detection and isolation/localization (LDI) systems. Usually, on the basis of measurements obtained from pressure and flow sensors at the inlet and outlet of a pipeline, specially designed state observers estimate intermediate fluid parameters; those parameters are compared with their predictions, and leaks can accordingly be detected.

An early application of nonlinear state observers to the detection and identification of a single leak in a pipeline is presented in [2]. This approach is further studied in [5] by considering an improved volume balancing method (for better estimation of the leak size), online estimation of the friction factor, the method of characteristic lines, and Kalman filtering. The problem of multiple-leak detection is discussed in [4, 14], while extension of the leak detection problem towards branched pipelines is presented in [15]. Other than the model-based methods of leak detection, there are approaches based on the pressure wave propagation

analysis in the time domain [11], the acoustic wave cross time-frequency spectrum analysis [8,9], the leak detection scheme based on rough set theory and support vector machine [10], to mention a few.

Practical implementation of a leak detection system, especially the model-based one, requires a numerical simulation of fluid flow on a (micro)computer. Therefore, the problem of limited computational resources arises. It motivates our investigations aimed at reduction of the computational overhead in simulations of the flow process in transmission pipelines.

The paper is organized as follows: Section 2 contains the derivation of a base discrete-time state-space model of the flow process in a pipeline. Section 3 presents a numerical rearrangement of the base model resulting in two systems of equations with tridiagonal matrices. Section 4 presents a comparison of the base and newly-derived models in terms of computational efficiency and accuracy. Section 5 provides final conclusions.

2 Base Model of the Flow Process

Let us consider the mathematical description of the pressure and mass-flow rate of liquid flowing in a transmission pipeline. It is expressed by two equations resulting from the momentum and mass conservation laws [2]:

$$\frac{A}{\nu^2}\frac{\partial p}{\partial t} + \frac{\partial q}{\partial z} = 0 \tag{1}$$

$$\frac{1}{A}\frac{\partial q}{\partial t} + \frac{\partial p}{\partial z} = -\frac{\lambda \nu^2}{2DA^2}\frac{q|q|}{p} - \frac{gsin\alpha}{\nu^2}p \tag{2}$$

where A is the cross-sectional area $[m^2]$, ν is the isothermal velocity of the sound in the fluid $[\frac{m}{s}]$, D is the diameter of the pipe $[m]$, q is the mass flow $[\frac{kg}{s}]$, p is the pressure $[Pa]$, t is the time $[s]$, z is the spatial coordinate $[m]$, λ is the dimensionless generalized friction factor, α is the inclination angle $[rad]$, and g is the gravitational acceleration $[\frac{m}{s^2}]$.

Since in practice the operation of a model-based algorithm for pipeline diagnosis may require simulation of the behavior of the underlying flow process. One way to get a solution is to apply the method of lines and solve the resulting system using an ODE solver [5]. In this paper the set of equations (1)–(2) is discretized for computer implementation. The pipeline is divided into N segments of equal length Δz, where the pressure at the end of each odd segment, and the flow rate at the end of each even segment, are computed. Mass-flow and pressure are computed at the inlet and outlet of the pipeline. The discretized pipeline, as defined above, is illustrated in Fig. 1.

The discrete-time model is derived by introducing low-order central difference schemes introduced in [1, 2]:

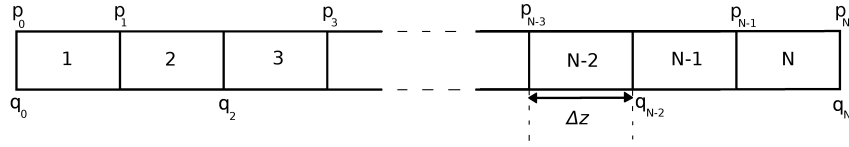$$\frac{\partial x}{\partial t} = \frac{3x_d^{k+1} - 4x_d^k + x_d^{k-1}}{2\Delta t} \tag{3}$$

Fig. 1. Discretization scheme of a pipeline with N segments

$$\frac{\partial x}{\partial z} = \frac{x_{d+1}^{k+1} - x_{d-1}^{k+1} + x_{d+1}^{k} - x_{d-1}^{k}}{4\Delta z} \tag{4}$$

where Δz is a spatial-step size, Δt is a time-step size, subscripts and superscripts denote the number of the pipeline segment and discrete-time index, respectively. The first differential scheme derived from the Taylor expansion provides a lower truncation error than the classic first-order difference scheme. The second equation represent the two-sided Crank-Nicolson scheme employed to minimize the error.

The substitution of (3)–(4) into the composed model (1)–(2) gives the following discretized set of equations for the flow process in the pipeline:

$$ap_d^{k+1} - b\left(q_{d-1}^{k+1} - q_{d+1}^{k+1}\right) = \frac{a}{3}\left(4p_d^k - p_d^{k-1}\right) + b\left(q_{d-1}^k - q_{d+1}^k\right) \tag{5}$$

$$b\left(p_{d+1}^{k+1} - p_{d-1}^{k+1}\right) + cq_d^{k+1} = b\left(p_{d-1}^k - p_{d+1}^k\right) + Y_d p_d^k + \left(\frac{4c}{3} + F_d^k\right)q_d^k - \frac{c}{3}q_d^{k-1} \tag{6}$$

where

$$a = \frac{3A}{2\nu^2 \Delta t}, \quad b = \frac{1}{4\Delta z}, \quad c = \frac{3}{2A\Delta t}, \quad Y_d = \frac{g\sin\alpha_d}{\nu^2}$$

and α_d denotes the inclination angle of a d-th segment. The nonlinear function F_d^k is approximated by

$$F_d^k \simeq -\frac{\lambda\nu^2}{DA}\frac{|q_d^k|}{p_{d-1}^k + p_{d+1}^k}$$

Rewriting (5)–(6) into the form of state-space equations, the model can be represented by the following compact state-space model:

$$\mathbb{A}\hat{\mathbf{x}}^k = \mathbb{B}\hat{\mathbf{x}}^{k-2} + \mathbb{C}\left(\hat{\mathbf{x}}^{k-1}\right)\hat{\mathbf{x}}^{k-1} + \mathbb{D}\mathbf{u}^{k-1} + \mathbb{E}\mathbf{u}^k \tag{7}$$

Taking into account nonsingularity of the recombination matrix [6], one obtains:

$$\hat{\mathbf{x}}^k = \mathbb{A}^{-1}\left(\mathbb{B}\hat{\mathbf{x}}^{k-2} + \mathbb{C}\left(\hat{\mathbf{x}}^{k-1}\right)\hat{\mathbf{x}}^{k-1} + \mathbb{D}\mathbf{u}^{k-1} + \mathbb{E}\mathbf{u}^k\right) \tag{8}$$

where $\mathbb{B}$ and $\mathbb{C}\left(\hat{\mathbf{x}}^{k-1}\right)$ are associated with the nonlinear dynamic of the state

$$\hat{\mathbf{x}}^k = \left[q_0^k\ q_2^k\ q_4^k \cdots q_N^k \,|\, p_1^k\ p_3^k\ p_5^k \cdots\ p_{N-1}^k\right]^T \in \mathbb{R}^{N+1}$$

and matrices $\mathbb{D}$ and $\mathbb{E}$ are associated with the input $\mathbb{u}^k = \begin{bmatrix} p_0^k\ p_N^k \end{bmatrix}^T \in \mathbb{R}^2$. Full description of these matrices can be found in [7].

As can be seen from (7) & (8), the singularity of $\mathbb{A}$ affects the model. This description is thus referred to as *singular state-space* model [16]. The term *singular* emphasizes the specific form of the model in which $\mathbb{A}$ may be not invertible in general. Moreover, the problem of singularity is quite complex, as our research shows that the model is very sensitive to the discretization parameters, which have to be aptly chosen in order to assure stability of the system. The matrix $\mathbb{A}$ is referred to as the recombination matrix and it is defined as

$$
\mathbb{A} = \left[\begin{array}{c|c} \mathbb{A}_1 & \mathbb{A}_2 \\ \hline \mathbb{A}_3 & \mathbb{A}_4 \end{array} \right] = \left[\begin{array}{c|c} \mathbb{D}_{\frac{N}{2}+1}(c) & \begin{matrix} \diagdown 2b & 0 & \cdots & 0 & 0 \\ -b & \diagdown b & \cdots & 0 & 0 \\ \vdots & & \ddots & & \vdots \\ 0 & 0 & \cdots & \diagdown b & 0 \\ 0 & 0 & \cdots & -b & \diagdown b \\ 0 & 0 & \cdots & 0 & -2b \end{matrix} \\ \hline \begin{matrix} -b & b & 0 & \cdots & 0 & 0 & 0 \\ 0 & -b & b & \cdots & 0 & 0 & 0 \\ \vdots & & \ddots & & & \vdots \\ 0 & 0 & 0 & \cdots & -b & b & 0 \\ 0 & 0 & 0 & \cdots & 0 & -b & b \end{matrix} & \mathbb{D}_{\frac{N}{2}}(a) \end{array} \right] \in \mathbb{R}^{(N+1)\times(N+1)}
$$

$$(9)$$

where $D_W(\theta) \in \mathbb{R}^{W \times W}$ denotes a diagonal matrix with θ on its diagonal. Note that the upper right submatrix is non-square and belongs to $\mathbb{R}^{\left(\frac{N}{2}+1\right)\times\left(\frac{N}{2}\right)}$.

Initial boundary conditions, required for calculating the subsequent values of the state vector in the first two steps, are obtained on the basis of available measurements at the time of the system's initialization. Linear distribution of both pressure and mass-flow along the pipe is assumed. The convergence of the solution, obtained with such boundary conditions, is satisfactory.

3   Model Reformulation

Sparsity of matrices in the state-space model (7) allows us to rearrange this model to a form which falls inside the scope of applicability of the Thomas algorithm [3], which reduces the computational complexity of computations.

The procedure starts with the consideration of the structure of submatrices in the recombination matrix. Two of them are square and diagonal, whereas the other two are non-square band matrices with the band width equal to 2:

$$
\mathbb{A}_1 = \mathbb{D}_{\frac{N}{2}+1}(c) \in \mathbb{R}^{\left(\frac{N}{2}+1\right)\times\left(\frac{N}{2}+1\right)} \tag{10}
$$

$$
\mathbb{A}_4 = \mathbb{D}_{\frac{N}{2}}(a) \in \mathbb{R}^{\frac{N}{2}\times\frac{N}{2}} \tag{11}
$$

$$
\mathbf{A}_2 = \begin{bmatrix} \diagdown 2b & 0 & \cdots & 0 & 0 \\ -b & \diagdown b & \cdots & 0 & 0 \\ \vdots & & \ddots & & \vdots \\ 0 & 0 & \cdots & \diagdown b & 0 \\ 0 & 0 & \cdots & -b & \diagdown b \\ 0 & 0 & \cdots & 0 & -2b \end{bmatrix} \in \mathbb{R}^{\left(\frac{N}{2}+1\right)\times\frac{N}{2}} \tag{12}
$$

$$
\mathbf{A}_3 = \begin{bmatrix} -b & \diagdown b & 0 & \cdots & 0 & 0 & 0 \\ 0 & -b & \diagdown b & \cdots & 0 & 0 & 0 \\ \vdots & & & \ddots & & & \vdots \\ 0 & 0 & 0 & \cdots & -b & \diagdown b & 0 \\ 0 & 0 & 0 & \cdots & 0 & -b & \diagdown b \end{bmatrix} \in \mathbb{R}^{\frac{N}{2}\times\left(\frac{N}{2}+1\right)} \tag{13}
$$

Matrices $\mathbf{A}_2$ and $\mathbf{A}_3$ as a pair have such a property that their multiplication (regardless of its order) results in tridiagonal matrices:

$$
\mathbf{A}_2\mathbf{A}_3 = \begin{bmatrix} -2b^2 & 2b^2 & 0 & 0 & 0 & & 0 & 0 & 0 \\ b^2 & -2b^2 & b^2 & 0 & 0 & \cdots & 0 & 0 & 0 \\ 0 & b^2 & -2b^2 & b^2 & 0 & & 0 & 0 & 0 \\ 0 & 0 & b^2 & -2b^2 & b^2 & & 0 & 0 & 0 \\ & & \vdots & & & \ddots & & \vdots & \\ 0 & 0 & 0 & & & b^2 & -2b^2 & b^2 & 0 & 0 \\ 0 & 0 & 0 & & & 0 & b^2 & -2b^2 & b^2 & 0 \\ 0 & 0 & 0 & \cdots & 0 & 0 & b^2 & -2b^2 & b^2 \\ 0 & 0 & 0 & & 0 & 0 & 0 & 2b^2 & -2b^2 \end{bmatrix} \in \mathbb{R}^{\left(\frac{N}{2}+1\right)\times\left(\frac{N}{2}+1\right)}
$$

$$
\tag{14}
$$

$$
\mathbf{A}_3\mathbf{A}_2 = \begin{bmatrix} -3b^2 & b^2 & 0 & 0 & 0 & & 0 & 0 & 0 \\ b^2 & -2b^2 & b^2 & 0 & 0 & \cdots & 0 & 0 & 0 \\ 0 & b^2 & -2b^2 & b^2 & 0 & & 0 & 0 & 0 \\ 0 & 0 & b^2 & -2b^2 & b^2 & & 0 & 0 & 0 \\ & & \vdots & & & \ddots & & \vdots & \\ 0 & 0 & 0 & & & b^2 & -2b^2 & b^2 & 0 & 0 \\ 0 & 0 & 0 & & & 0 & b^2 & -2b^2 & b^2 & 0 \\ 0 & 0 & 0 & \cdots & 0 & 0 & b^2 & -2b^2 & b^2 \\ 0 & 0 & 0 & & 0 & 0 & 0 & b^2 & -3b^2 \end{bmatrix} \in \mathbb{R}^{\left(\frac{N}{2}+1\right)\times\frac{N}{2}}.
$$

$$
\tag{15}
$$

Thus, the following lemma can be formulated:

Lemma 1. *Both matrices obtained from multiplications $\mathbf{A}_2\mathbf{A}_3$ and $\mathbf{A}_3\mathbf{A}_2$ are tridiagonal.*

In order to achieve a simpler form of the model, the right-hand side of (7) is represented by an auxiliary vector:

$$\mathbf{w}\left(\hat{\mathbf{x}}^{k-1}, \hat{\mathbf{x}}^{k-2}, \mathbf{u}^{k}, \mathbf{u}^{k-1}\right) = \mathbb{B}\hat{\mathbf{x}}^{k-2} + \mathbb{C}\left(\hat{\mathbf{x}}^{k-1}\right)\hat{\mathbf{x}}^{k-1} + \mathbb{D}\mathbf{u}^{k-1} + \mathbb{E}\mathbf{u}^{k}. \quad (16)$$

Hence, (7) is rewritten as:

$$\mathbb{A}\hat{\mathbf{x}}^{k} = \mathbf{w}\left(\hat{\mathbf{x}}^{k-1}, \hat{\mathbf{x}}^{k-2}, \mathbf{u}^{k}, \mathbf{u}^{k-1}\right). \quad (17)$$

Since the matrix $\mathbb{B}$ is diagonal and the matrices $\mathbb{C}$, $\mathbb{D}$ and $\mathbb{E}$ are sparse [7], computation of the vector $\mathbf{w}$ is of complexity $\mathcal{O}(N)$. Hence, one can rewrite (16) taking into account the division of the recombination matrix into four submatrices:

$$\left[\begin{array}{c|c} \mathbb{A}_1 & \mathbb{A}_2 \\ \hline \mathbb{A}_3 & \mathbb{A}_4 \end{array}\right] \hat{\mathbf{x}}^{k} = \mathbf{w}. \quad (18)$$

Since

$$\hat{\mathbf{x}}^{k} = \begin{bmatrix} \mathbf{q}^{k} \\ \mathbf{p}^{k} \end{bmatrix} \quad \text{and} \quad \mathbf{w} = \begin{bmatrix} \mathbf{g} \\ \mathbf{h} \end{bmatrix}$$

where $\mathbf{q}^{k}, \mathbf{g} \in \mathbb{R}^{\frac{N}{2}+1}$ and $\mathbf{p}^{k}, \mathbf{h} \in \mathbb{R}^{\frac{N}{2}}$, (18) is shown as a system of equations:

$$\mathbb{A}_1\mathbf{q}^{k} + \mathbb{A}_2\mathbf{p}^{k} = \mathbf{g} \quad (19)$$

$$\mathbb{A}_3\mathbf{q}^{k} + \mathbb{A}_4\mathbf{p}^{k} = \mathbf{h}. \quad (20)$$

Solving it for $\mathbf{q}^{k}$ and $\mathbf{p}^{k}$ leads to:

$$\mathbf{q}^{k} = \mathbb{A}_1^{-1}\left(\mathbf{g} - \mathbb{A}_2\mathbf{p}^{k}\right) \quad (21)$$

$$\mathbf{p}^{k} = \mathbb{A}_4^{-1}\left(\mathbf{h} - \mathbb{A}_3\mathbf{q}^{k}\right) \quad (22)$$

Because $\mathbb{A}_1$ and $\mathbb{A}_4$ used in (21)–(22) are diagonal matrices with identical diagonal elements, the effect of the pre-multiplication of the respective vectors by a matrix inversion, can be expressed as the division of these vectors by a respective number. By defining: $\tilde{\mathbf{g}} = \frac{\mathbf{g}}{c}$, $\tilde{\mathbb{A}}_2 = \frac{\mathbb{A}_2}{c}$, $\tilde{\mathbf{h}} = \frac{\mathbf{h}}{a}$ and $\tilde{\mathbb{A}}_3 = \frac{\mathbb{A}_3}{a}$, one obtains:

$$\mathbf{q}^{k} = \tilde{\mathbf{g}} - \tilde{\mathbb{A}}_2\mathbf{p}^{k} \quad (23)$$

$$\mathbf{p}^{k} = \tilde{\mathbf{h}} - \tilde{\mathbb{A}}_3\mathbf{q}^{k} \quad (24)$$

Substituting (24) into (23) and vice versa, results in

$$\mathbf{q}^{k} = \tilde{\mathbf{g}} - \tilde{\mathbb{A}}_2\tilde{\mathbf{h}} + \tilde{\mathbb{A}}_2\tilde{\mathbb{A}}_3\mathbf{q}^{k} \quad (25)$$

$$\mathbf{p}^{k} = \tilde{\mathbf{h}} - \tilde{\mathbb{A}}_3\tilde{\mathbf{g}} + \tilde{\mathbb{A}}_3\tilde{\mathbb{A}}_2\mathbf{p}^{k} \quad (26)$$

These equations can be consequently rearranged to:

$$\left(\mathbb{I} - \tilde{\mathbf{A}}_2\tilde{\mathbf{A}}_3\right)\mathbf{q}^k = \tilde{\mathbf{g}} - \tilde{\mathbf{A}}_2\tilde{\mathbf{h}} \tag{27}$$

$$\left(\mathbb{I} - \tilde{\mathbf{A}}_3\tilde{\mathbf{A}}_2\right)\mathbf{p}^k = \tilde{\mathbf{h}} - \tilde{\mathbf{A}}_3\tilde{\mathbf{g}} \tag{28}$$

Taking advantage of the previously defined Lemma 1, the results of the matrix multiplications $\tilde{\mathbf{A}}_3\tilde{\mathbf{A}}_2$ and $\tilde{\mathbf{A}}_2\tilde{\mathbf{A}}_3$ are tridiagonal, as well as (since we subtract these matrices from the identity matrix) the expressions $\left(\mathbb{I} - \tilde{\mathbf{A}}_3\tilde{\mathbf{A}}_2\right)$ and $\left(\mathbb{I} - \tilde{\mathbf{A}}_2\tilde{\mathbf{A}}_3\right)$ are also tridiagonal matrices. Hence, the Thomas algorithm [12] can be applied assuring the computational complexity of order $\mathcal{O}(N)$ [3]. The algorithm is defined for equations given in the following form:

$$\mathbb{T}\mathbf{v} = \mathbf{d} \tag{29}$$

where $\mathbf{v}$ and $\mathbf{d}$ are vectors, and $\mathbb{T}$ is a tridiagonal parameter matrix of the following structure:

$$\mathbb{T} = \begin{bmatrix} \beta_1 & \gamma_1 & & & \mathbf{0} \\ \alpha_2 & \beta_2 & \gamma_2 & & \\ & \alpha_3 & \ddots & \ddots & \\ & & \ddots & \ddots & \gamma_{n-1} \\ \mathbf{0} & & & \alpha_n & \beta_n \end{bmatrix}. \tag{30}$$

Efficient computation of the vector $\mathbf{v}$ is based on LU decomposition of the tridiagonal matrix $\mathbb{T} = \mathbb{L}\mathbb{U}$, resulting in the following lower and upper triangular matrices [3]:

$$\mathbb{L} = \begin{bmatrix} 1 & & & & \mathbf{0} \\ l_2 & 1 & & & \\ & \ddots & \ddots & & \\ & & l_{n-1} & 1 & \\ \mathbf{0} & & & l_n & 1 \end{bmatrix} \quad \mathbb{U} = \begin{bmatrix} u_1 & r_1 & & & \mathbf{0} \\ & u_2 & r_2 & & \\ & & \ddots & \ddots & \\ & & & u_{n-1} & r_{n-1} \\ \mathbf{0} & & & & u_n \end{bmatrix}. \tag{31}$$

Consequently, equation (29) can be shown as $\mathbb{L}\mathbb{U}\mathbf{v} = \mathbf{d}$. For the purpose of calculating the vector $\mathbf{v}$ for a known $\mathbf{d}$, we can solve subsequently two matrix equations: $\mathbb{L}\mathbf{y} = \mathbf{d}$ and $\mathbb{U}\mathbf{v} = \mathbf{y}$, with initial condition $u_1 = \beta_1, y_1 = d_1$, according to the following equations:

$$l = \frac{\alpha_i}{u_{i-1}}, \quad u_i = \beta_i - l\gamma_{i-1}, \quad y_i = d_i - ly_{i-1}, \quad \text{for } i = 1, 2, 3, ..., n \tag{32}$$

$$v_n = \frac{y_n}{u_n}, \quad v_i = \frac{y_i - \gamma_i v_{i+1}}{u_i}, \quad \text{for } i = n-1, n-2, ..., 2, 1. \tag{33}$$

It can be shown that the tridiagonal matrices $\left(\mathbb{I} - \tilde{\mathbf{A}}_3\tilde{\mathbf{A}}_2\right)$ and $\left(\mathbb{I} - \tilde{\mathbf{A}}_2\tilde{\mathbf{A}}_3\right)$ are diagonally dominant, therefore, the Thomas algorithm can successfully solve (27)–(28) for $\mathbf{q}^k$ and $\mathbf{p}^k$, respectively [3]. Then, combining both vectors into a common state vector, a single iteration of the simulation is completed. The simulated model with this state vector, obtained using the algorithm (32)–(33), is called the analytic Thomson method (ATM).

4 Comparison of the Methods

There are two principal criteria for comparing the models: the computation time, and the accuracy of the results. A gain in computational time is strictly connected with the ability to simulate the flow process in an on-line manner, which is usually determined by the set of physical parameters and the selected discretization grid. The accuracy of the model tells, whether the results obtained by the base model and the ATM model are similar, and thus, whether the same leak detection methods can be applied using both models. The boundary conditions were calculated assuming linear pressure and flow distributions along the pipeline, based on available measurements at the inlet and outlet of the monitored pipeline. The spatial step is closely related to the length of the pipeline and the number of segments, while the time step was calculated using the method described in [7] to provide a maximum margin of stability.

4.1 Computation Time

The computation time is analyzed using the MATLAB environment with built-in functions to measure the execution time associated with both methods. The results, presented as the ratio of the base model computation time to the ATM computation time, are referred to as the computational speedup and presented in Fig. 2. Note that all matrices are stored as full tables. It is necessary to carry out further research (of the considered methods) for sparse matrices.

Note that for sparse discretization, both methods have similar computation time. However, the finer discretization the more significant computational speedup of the ATM with respect to the base method (e.g., the former becomes approximately 15 times faster than the latter for 200 segments).

4.2 Validity of the ATM Model

The second analysis concerns the validity of the ATM model. Since the base model has already been validated [2], a measure for the ATM model accuracy can be the maximum value (for the whole simulation) of the normalized second
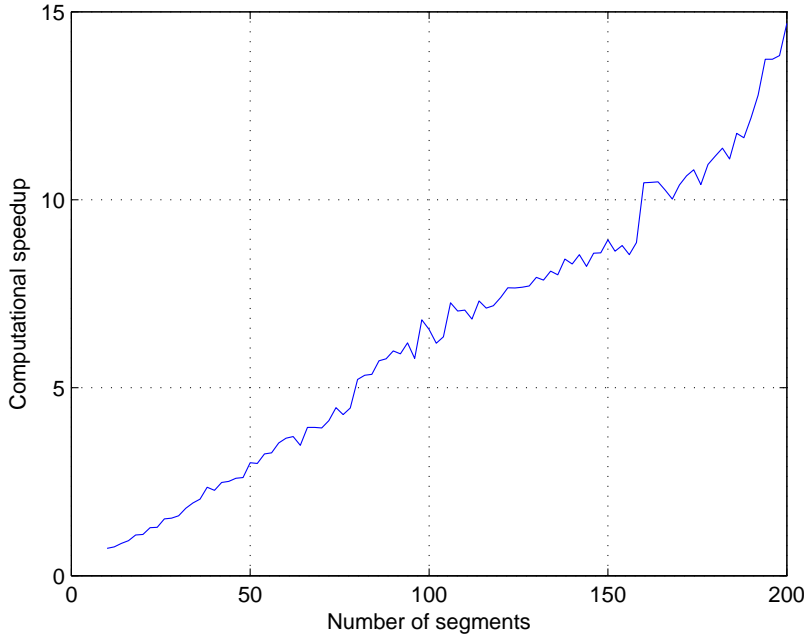
Fig. 2. Computational speedup measured as the ratio of the base-model computation time to the ATM computation time (in this experiment the execution times were measured for 5000 iterations simulating the pipeline, and the physical parameters of the flow were the following: L=75 [km], D=0.67 [m], λ=0.02, ν=300 [ms], p_{inlet}=10 [MPa], and p_{outlet}=8 [MPa])

norm of the difference between the two respective state vectors. The results are presented in Fig. 3.

Since the coordinates of the state-space vector which concern the pressure were of the order of magnitude 10^6, due to input pressure, the norm is scaled with respect to the base-model state vector norm. As a result, the measure of the difference M_d between the models has been calculated as:

$$M_d = 20 \log_{10} \left(\frac{\max_k ||\hat{\mathbf{x}}_{\mathbf{b}}^{\mathbf{k}} - \hat{\mathbf{x}}_{\mathbf{atm}}^{\mathbf{k}}||}{\max_k ||\hat{\mathbf{x}}_{\mathbf{b}}^{\mathbf{k}}||} \right) \quad [\text{dB}] \tag{34}$$

where $\hat{\mathbf{x}}_{\mathbf{b}}^{\mathbf{k}}$ and $\hat{\mathbf{x}}_{\mathbf{atm}}^{\mathbf{k}}$ denote the state vectors of the base and ATM models, respectively.

Apart from the influence of the spatial discretization on the model accuracy, the influence of the temporal discretization has also been examined. The μ coefficient used in the relation $\Delta t = \mu \frac{\Delta z}{c}$, is determined by the time- and spatial-step sizes and the sound velocity. Results, being a scaled second norm of the differ-
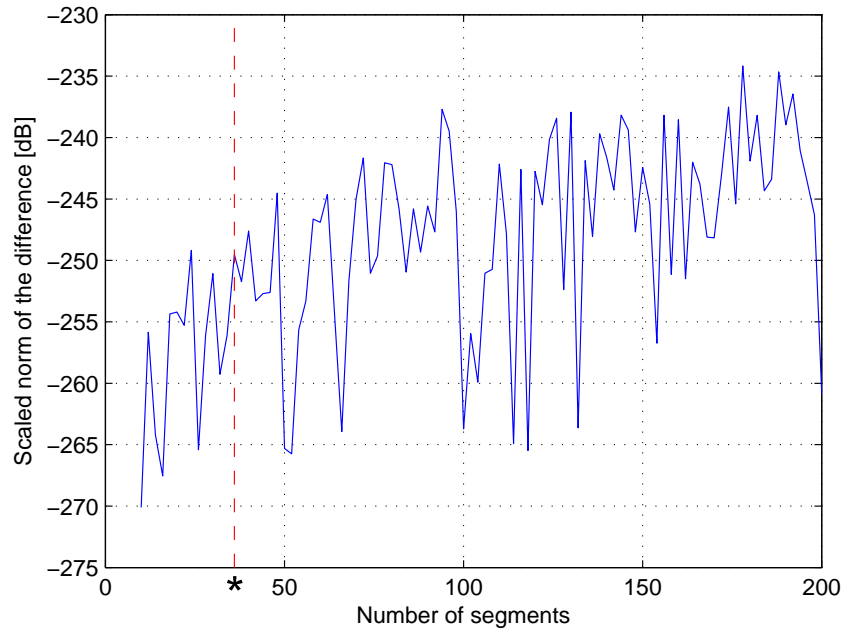
Fig. 3. Scaled second norm of the difference between two state vectors obtained using the base model and the ATM model (number of iterations was 5000, and the physical parameters of the flow were as follows: L=75 [km], D=0.67 [m], λ=0.02, ν=300 [ms], p_{inlet}=10 [MPa], and p_{outlet}=8 [MPa])

ence between the state vectors, are presented in Fig. 4, for a fixed N=36 (see * in Fig. 3), and equivalently Δz= 2083 [m], as a function of μ (or equivalently Δt in this setting).

The increase of μ causes a clear decrease of the state difference between the two models, which varies between -275 dB and -235 dB in Fig. 4. Since the numerical noise level is around -300 dB, the difference between models is negligible. However, the computational overhead is significantly reduced when the ATM model is applied.

5 Conclusions

The paper addresses the problem of computational complexity of the numerical computation and simulation of the flow process in transmission pipelines. The state-space model has been rearranged in order to obtain two equations with tridiagonal matrices, for which the Thomas method can be applied. Hence, the computational overhead is reduced, while the simulation results remain close to the ones resulting from the base model. The computational speedup is evident
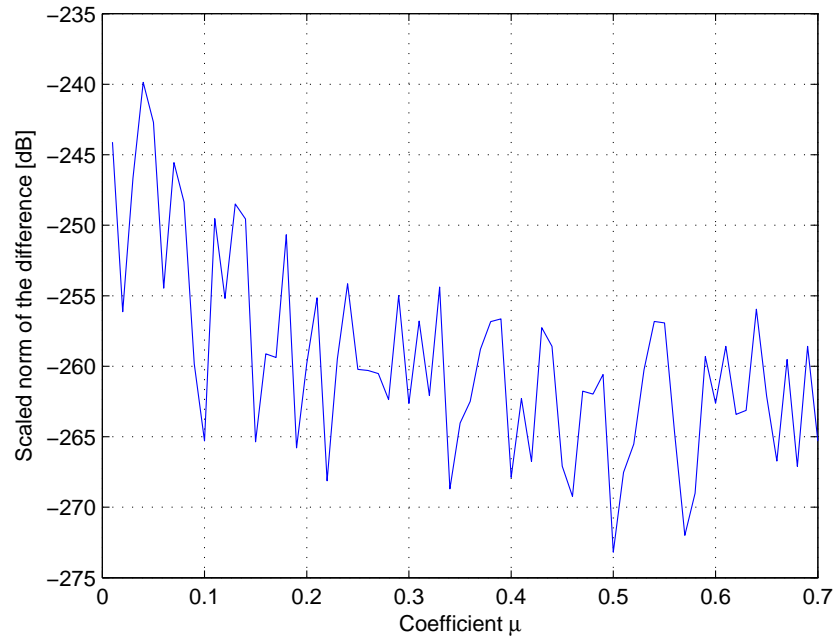
Fig. 4. Scaled second norm of the difference between two state vectors obtained using the base model and the ATM model (number of iterations was 5000, and the physical parameters of the flow were as follows: L=25 [km], N=36, D=0.4 [m], λ=0.02, ν=304 [ms], p_{inlet}=3.2 [MPa], and p_{outlet}=3 [MPa])

for a fine discretization of a pipeline. Due to the small difference between the state vectors, both models can be considered equivalent, and therefore the leak detection methods can be evenly well applied using both the state-space models.

There is a possibility that the algorithm can become unstable due to an incorrect choice of the discretization grid (this issue is discussed in details in [7], where a certain restriction, in the form of an inequality, on the choice of the discretization grid is precisely provided). Respective study shows that both models become unstable in the same circumstances, so there is no definite profit of one over another in terms of stability.

References

1. Billmann, L.: Studies on improved leak detection methods for gas pipelines. Internal Report. Institut fur Regelungstechnik TH-Darmstadt (1982)

2. Billmann, L., Isermann, R.: Leak detection methods for pipelines. Automatica, 23(3), 381–385 (1987)
3. Conte, S.D., de Boor, C.: Elementary Numerical Analysis: An Algorithmic Approach, (third ed.). McGraw-Hill (1980)
4. Delgado-Aguiñaga, J.A., Besançon, G., Begovich, O., Carvajal, J.E.: Multi-leak diagnosis in pipelines based on Extended Kalman Filter. Control Engineering Practice, Volume 49, p. 139–148. http://dx.doi.org/10.1016/j.conengprac.2015.10.008 (2016)
5. Gunawickrama, K.: Leak Detection Methods for Transmission Pipelines, (PhD Thesis supervised by Z. Kowalczuk). Gdańsk Univeristy of Technology, Gdańsk (2001)
6. Kowalczuk, Z., Tatara, M.: Analytical modeling of flow processes: Analysis of computability of a state-space model. In: XI Int. Conf. on Diagnostics of Processes and Systems, 8-11 September 2013, pages 74.1–12. Łagów Lubuski (2013)
7. Kowalczuk, Z., Tatara, M.: Approximate models and parameter analysis of the flow process in transmission pipelines. In: Advanced and Intelligent Computations in Diagnosis and Control, pp. 239–252 (2016)
8. Li, S., Wen, Y., Li, P., Yang, J., Dong, X., Mu, Y.: Leak location in gas pipelines using cross-time-frequency spectrum of leakage-induced acoustic vibrations. Journal of Sound and Vibration, 333(17), 3889–3903. https://doi.org/10.1016/j.jsv.2014.04.018 (2014)
9. Li, S., Zhang, J., Yan, D., Wang, P., Huang, Q., Zhao, X., Cheng, Y., Zhou, Q., Xiang, N., Dong, T.: Leak detection and location in gas pipelines by extraction of cross spectrum of single non-dispersive guided wave modes. Journal of Loss Prevention in the Process Industries, 44, 255–262. https://doi.org/10.1016/j.jlp.2016.09.021 (2016)
10. Mandal, S. K., Chan, F. T. S., Tiwari, M. K.: Leak detection of pipeline: An integrated approach of rough set theory and artificial bee colony trained SVM. Expert Systems with Applications, 39(3), 3071–3080. https://doi.org/10.1016/j.eswa.2011.08.170 (2012)
11. Ostapkowicz, P., Bratek, A.: Leak detection in liquid transmission pipelines during transient state related to a change of operating point. In: Kowalczuk Z, (Ed.): Advanced and Intelligent Computations in Diagnosis and Control, pp. 253–65. Switzerland: Springer International Publishing (2016)
12. Thomas, L. H.: Elliptic problems in linear difference equations over a network. New York: Watson Sci. Comput. Lab. Rept., Columbia University (1949)
13. Torres, L., Besançon, G., Verde, C.: Leak detection using parameter identification. In: The 8th IFAC Symposium SAFEPROCESS-2012, Mexico City, Mexico (2012)
14. Verde, C., Visairo, N., Gentil, S.: Two leaks isolation in a pipeline by transient response. Advances in Water Resources, vol. 30, issue 8, pp. 1711–1721 (2007)
15. Verde, C., Torres, L.: Referenced model based observers for leaks' location in a branched pipeline, The 9th International Federation of Automatic Control (IFAC) Symposium SAFEPROCESS-2015, Paris, France (2015)
16. Verghese, G., Levy, B., Kailath, T.: A generalized state-space for singular systems. IEEE Transactions on Automatic Control, vol. 26, issue 4 (1981)